

Recent theoretical studies of beam crystallization

Jie Wei

BNL (USA) and IHEP (China)

H. Okamoto, H. Sugimoto

Hiroshima University (Japan)

Y. Yuri

JAEA (Japan)

A.M. Sessler

LBNL (USA)

COOL'07 Workshop, September 10 - 14, 2007



BROOKHAVEN
NATIONAL LABORATORY

中国科学院高能物理研究所
Institute of High Energy Physics
Chinese Academy of Sciences

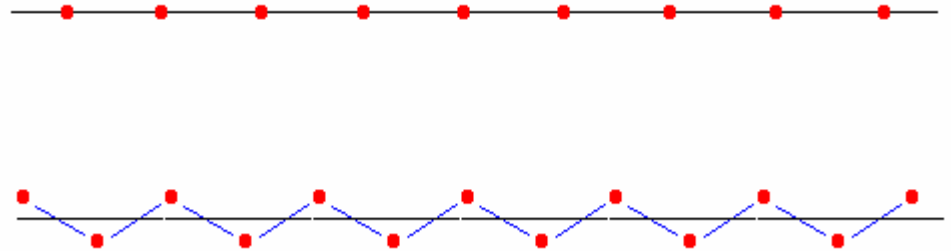
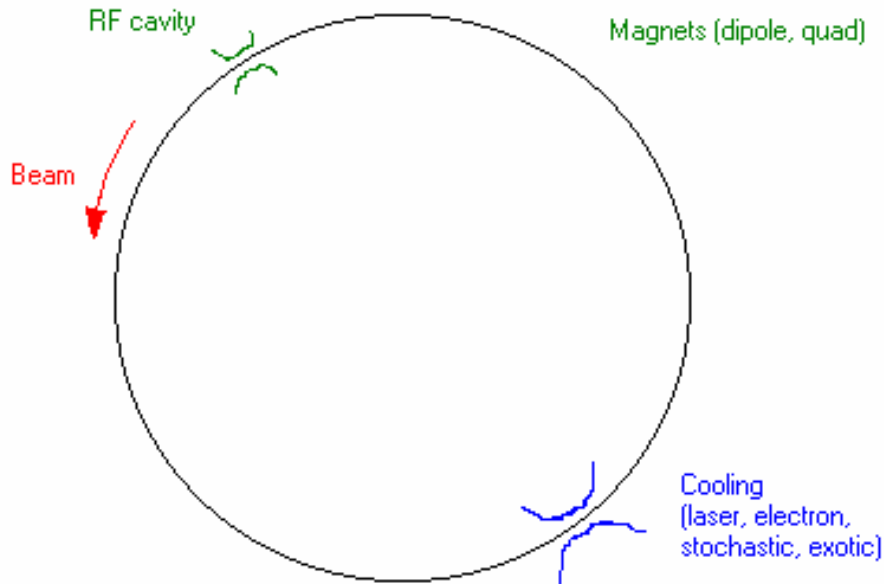
Outline

- Introduction
- Colliding crystals
 - Rare ion collider with ordered ions
 - Electron-ion collider with an ordered ion beam
- Lattices for attaining high energy crystals
 - High/imaginary transition-energy lattices
- Phonon theories for crystal stability study
 - Analytical evaluation under smooth approximation (3D)
 - Analytical evaluation for actual machine lattice (1D)
- Molecular dynamics study of high energy crystal
- Examples and discussion

Acknowledgements: X.P. Li, S. Machida, D. Moehl, D. Trbojevic ...

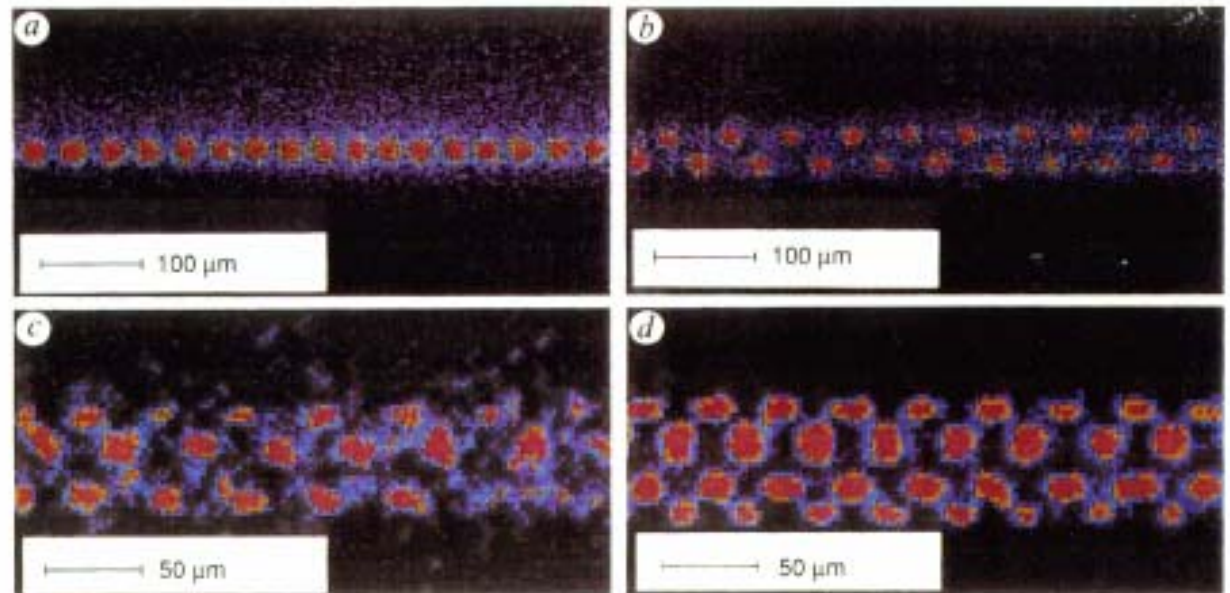
What is a crystalline beam?

- Near-zero emittance beam
- Highest possible beam density
- Highest possible beam luminosity
- Ordered particle distribution (one-component Coulomb crystal) as a new state of matter



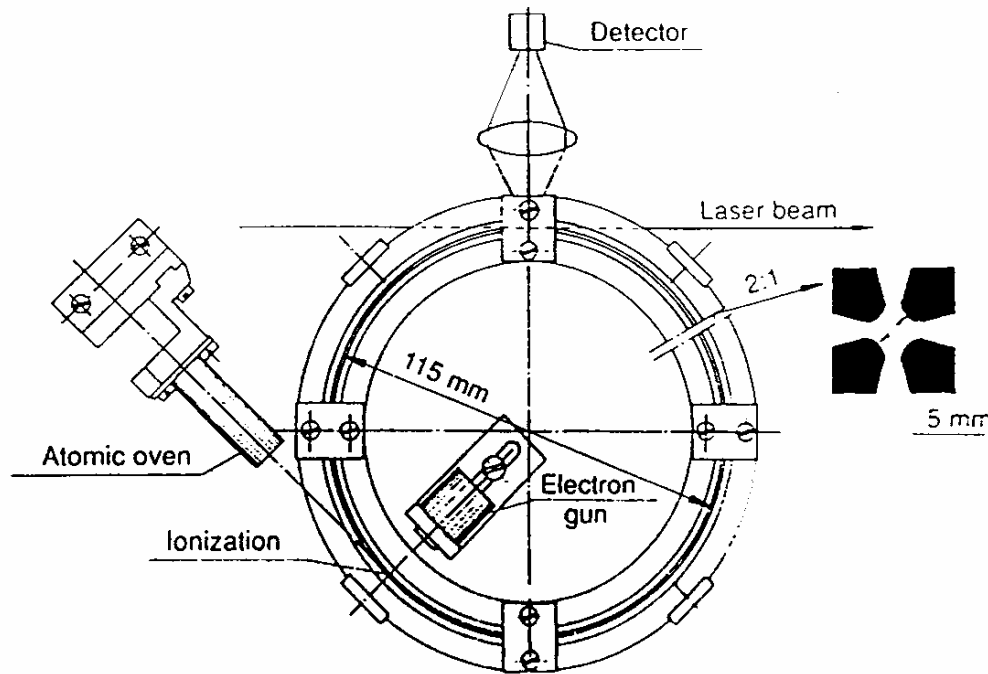
Coulomb crystals observed in traps

FIG. 2 Colour-coded images of crystalline structures of laser-cooled $^{24}\text{Mg}^+$ ions. The intensity increases from violet to blue, yellow and red. Individual ions could be resolved in these images. The ions arrange themselves in minimum energy configurations. *a* For low ion density ($\lambda = 0.29$) the ions form a string along the field axis; *b*, increasing the ion density changes the configuration to a zig-zag ($\lambda = 0.92$). At still higher ion densities the ions form ordered helical structures on the surface of a cylinder: *c*, two interwoven helices at $\lambda = 1.9$; *d* three interwoven helices at $\lambda = 2.6$. Experimental images are displayed above, visualizations below.



NATURE · VOL 357 · 28 MAY 1992

RFQ ring schematic layout



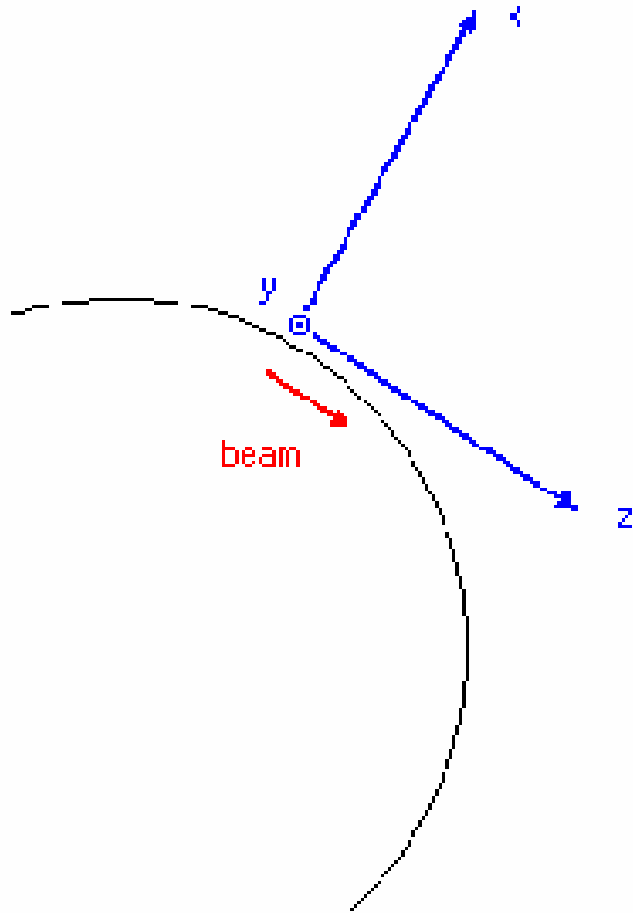
- Stationary $^{24}\text{Mg}^+$ ions
- Table top trap
- Multi-layer structure observed
- Structure in agreement with classical prediction

FIG. 1 Quadrupole storage ring, with the atomic beam oven and electron gun. The storage ring consists of four circular electrodes, and the diameter of the toroidal storage volume is $2R=115$ mm. The insert shows an enlarged cross-section with opposite electrodes having a separation of $2r_0=5$ mm. The laser beam enters the storage volume tangentially. Resonance fluorescence is detected with a photomultiplier tube or an imaging photon detector system.

Brief history

- 1980: Novosibirsk group (Dement'ev et al) saw anomaly in e-cooled proton beam; proposing crystalline beam concept
- 1986: Schiffer, Rahman, Hasse et al started theoretical study with the molecular dynamics method
 - Kienle, Habs, Hasse, Avilov, Hofmann, Hangst, Poulsen ...
- 1987: Diedrich et al; Gilbert et al; Walther ... experimental observation of Coulomb crystals in various kinds of traps
- 1993: Wei, Li, Sessler obtained conditions for crystallization & maintenance in actual storage rings
- More current works:
 - GSI group (Steck et al) observed 1-D ordering in beam
 - Heidelberg, Aarhus groups on experimental laser cooling
 - Okamoto et al on theoretical study of 3-D laser cooling
 - Noda, Ikegami, et al commissioning S-LSR and dispersion-free ring
 - Meshkov, Katayama, Moehl et al on colliding 1D strings for rare ions

Molecular dynamics approaches



- Use beam rest frame:
 - Non-relativistic motion of particles
 - Easy to adopt the molecular dynamics methods
 - Crystallization: zero temperature
- Derivation of equations of motion:
 - Use general relativity formalism -- EOM in tensor forms
 - Find the coordinate system transformation
 - Transform the EOM from lab frame to the beam rest frame
- Use Molecular Dynamics methods

•J. Wei, "General relativity derivation of beam rest-frame Hamiltonian", Proc. Particle Accelerator Conference, Chicago, 1678-1680 (2001)

•J. Wei, X.-P. Li, A.M. Sessler, BNL Report 52381 (1993); PAC'93, 3527 (1993)

A view from the beam rest frame

- Particle motion in the beam rest frame

$$H = \begin{cases} \frac{1}{2} (P_x^2 + P_y^2 + P_z^2) + \frac{1}{2} x^2 - \gamma x P_z + V_C & \text{(bending section)} \\ \frac{1}{2} (P_x^2 + P_y^2 + P_z^2) - \frac{n_1}{2} (x^2 - y^2) + V_C + U_s & \text{(straight section)} \end{cases}$$

- Coulomb interaction among particles

$$V_C = \sum_j \frac{1}{\sqrt{(x_j - x)^2 + (y_j - y)^2 + (z_j - z)^2}}$$

- Transformed Hamiltonian

$$H(x_\beta, P_x, y_\beta, P_y, z, P_z, \tau) = \frac{P_x^2}{2} + \frac{K_x(\tau)x_\beta^2}{2} + \frac{P_y^2}{2} + \frac{K_y(\tau)y_\beta^2}{2} + \frac{1 - \gamma^2 F_z(\tau)}{2} P_z^2 + V_C(x, y, z)$$

$$F_z = \begin{cases} D + DD'' + D'^2 & \text{(bends)} \\ DD'' + D'^2 & \text{(straights)} \end{cases} \quad \langle F_z \rangle = \frac{1}{\gamma_t^2}$$

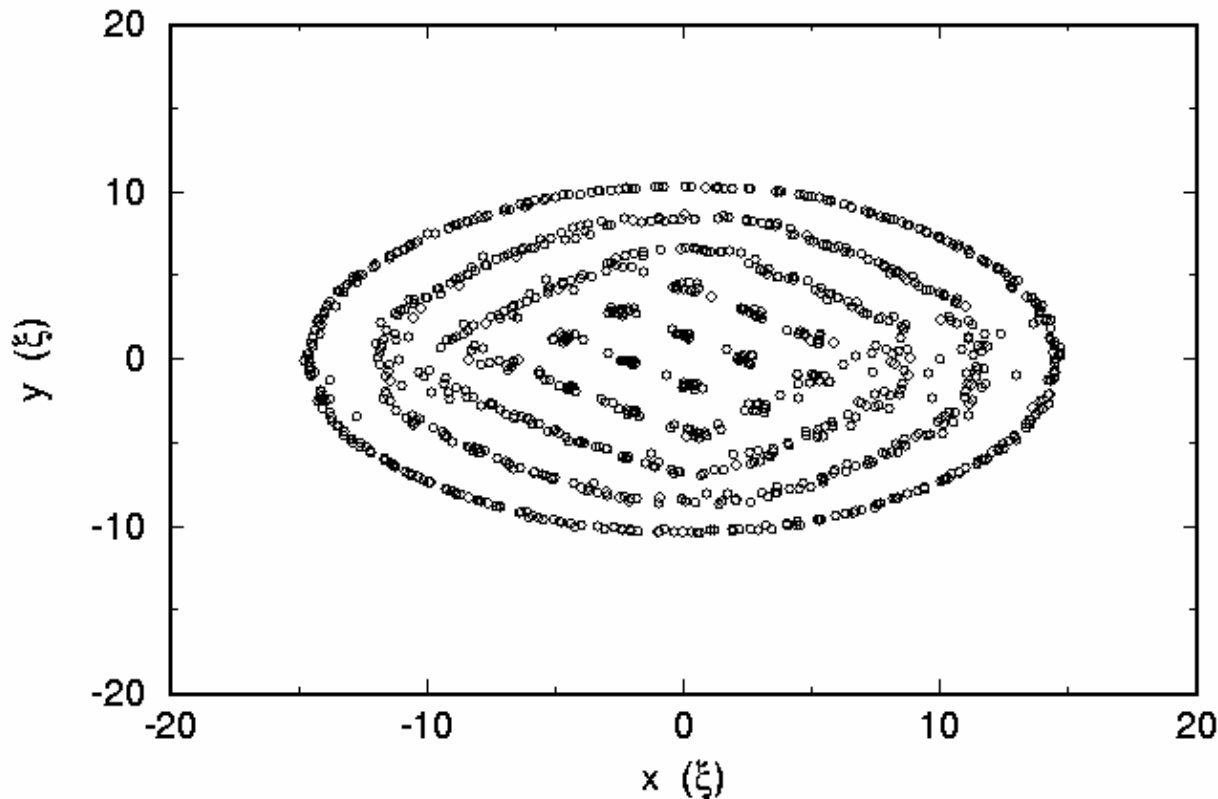
- Time-dependent Hamiltonian in beam rest frame

Basic properties of crystalline beams

- In general, the Hamiltonian is explicitly time-dependent (AG focusing); system is not conserved
 - Beam heats up when resonance conditions are met
 - Strongest (linear) resonance: lattice freq. = 2 x crystal phonon frequency
- Above transition energy: negative mass regime - Hamiltonian is not positive definite
 - Growth in all directions regardless of resonance conditions

- Conditions for crystallization:
 - Ring must operate below the transition energy
 - Phase advance per lattice super-period must not exceed 127° (preferably $< 90^\circ$)

Multi-layer beam simulated in actual ring



- Characteristic distance:

$$\xi = \left(\frac{r_0 \rho^2}{\beta^2 \gamma^2} \right)^{1/3}$$

- (1 -- 100 μm)

- Typical (lab frame) inter-particle distance:

$$\Delta = 1.6 \xi \gamma^{-1} v_{\text{eff}}^{-2/3}$$

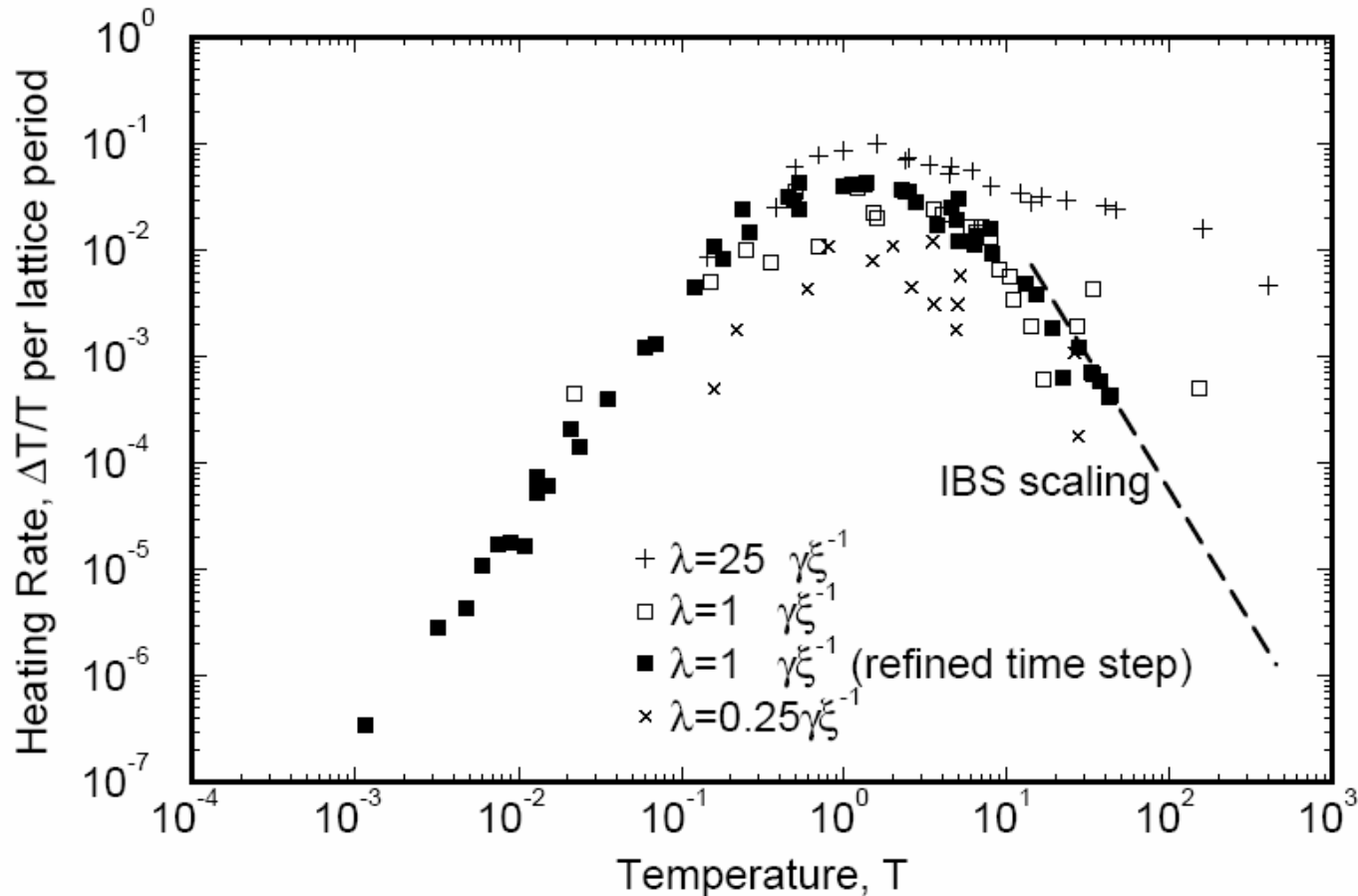
$$v_{\text{eff}}^2 = \min(v_y^2, v_x^2 - \gamma^2)$$

- Highest density:

$$\lambda_{\text{ave}} = \frac{\beta^2 \gamma^3 v_{\text{ave}}^2}{2 r_0 \rho^2}$$

Heating not predictable by usual IBS theory

- Finest level, particle-on-particle interaction
- Predicts a growth-rate turn-over when the beam is cooled towards the crystalline state



Motivation of new studies (from co-authors)

- In order to get a Ph. D degree -- Sugimoto
- To impress my supervisor at JAEA -- Yuri
- Just to have fun – Professor Okamoto
- To justify coming to this workshop – Wei
- An easy subject suitable for an old man - Sessler

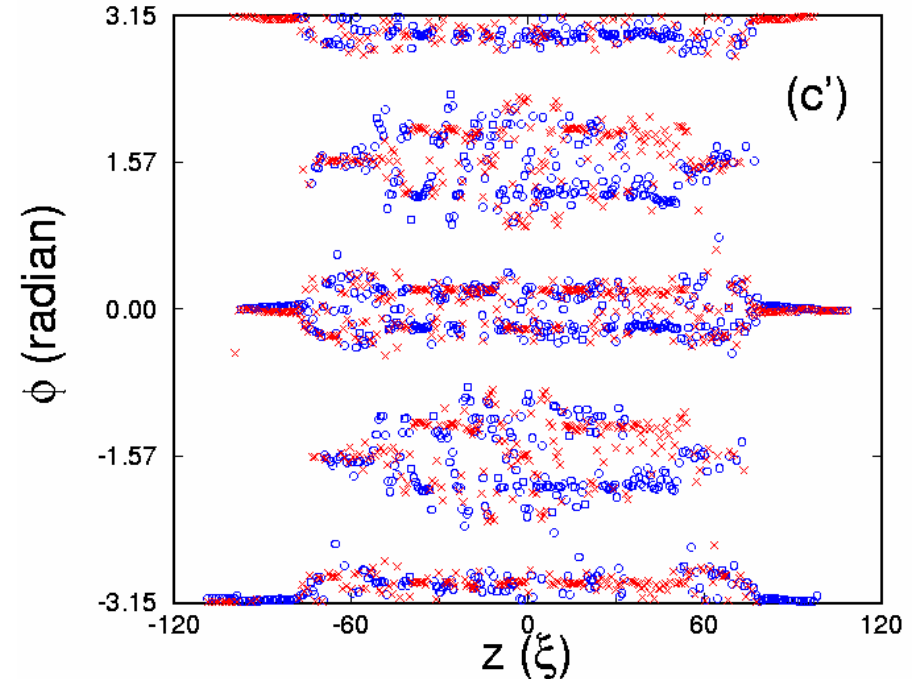
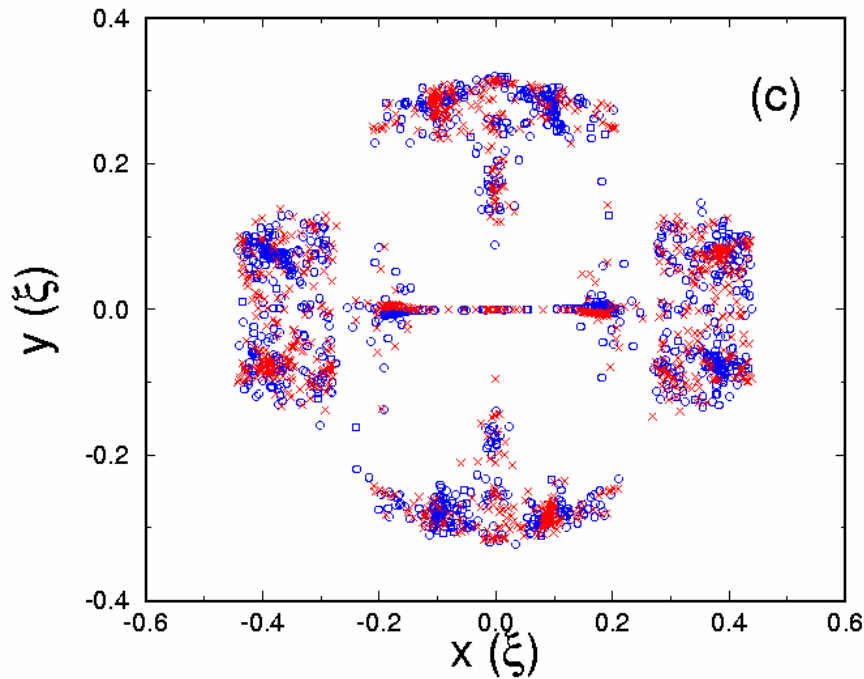
Motivation to study colliding beams

- Study potential benefits of ordered beam in a collider
 - Greatly enhanced luminosity; overriding beam-beam limits
 - » Issue 1: can crystals be formed at very high energies?
 - » Issue 2: are event rate / burn rate too high for detectors?
 - » Issue 3: how to practically cool the beam?
 - Achieve useable luminosity with very small number of ions (rare ion collider – Meshkov, Katayama, Moehl et al)
 - » Rare-ion collider with ordered ions in a RHIC-like ring
 - » Electron-ion collider with ordered ions (RIKEN studies)
- Study lattices appropriate for beams at high energies
 - High/imaginary transition lattices satisfying known conditions
- Develop phonon theories to compliment MD simulation

Overcoming beam-beam limit

- Strength of Coulomb restoring force
 - “incoherent space charge” tune shift \sim Tune ν_{xy}
- Regime of luminosity enhancement
 - “beam-beam” tune shift $<$ “incoherent space charge” tune shift
 $\rightarrow \sim 1$
 - In the absence of ordering, beam-beam limit ~ 0.01
- Significant enhancement of luminosity
 - $\sim 10^4$

Collision of ordered beam - MD simulation



- "incoherent space charge" tune shift ~ -3.8
- "beam-beam tune shift" ~ -0.27

Lattices for attaining high-energy crystals

- Can we form crystals at energies (γ) much higher than machine tune (v_x, v_y)?
- Lattice candidates
 - High transition energy ($\gamma_T \gg v_x$) lattice
 - Imaginary transition energy ($\gamma_T^2 < 0$)
- Do they satisfy the maintenance condition?

Missing-dipole 3-cell lattice

- High transition, but violating the maintenance condition

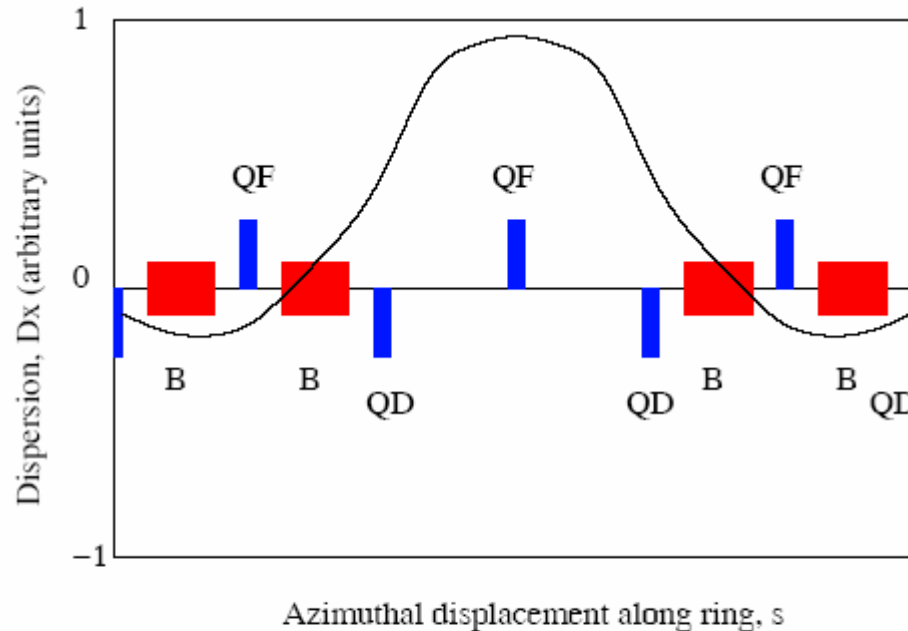


Figure 1: 3-cells missing-dipole low-momentum-compaction lattice module. B, QF, and QD denote dipole, focusing, and defocusing quadrupole magnets, respectively. The horizontal phase advance across the module is approximately 270° .

Negative-bend lattice

- Satisfy all known conditions; capable for both high and imaginary transition energies

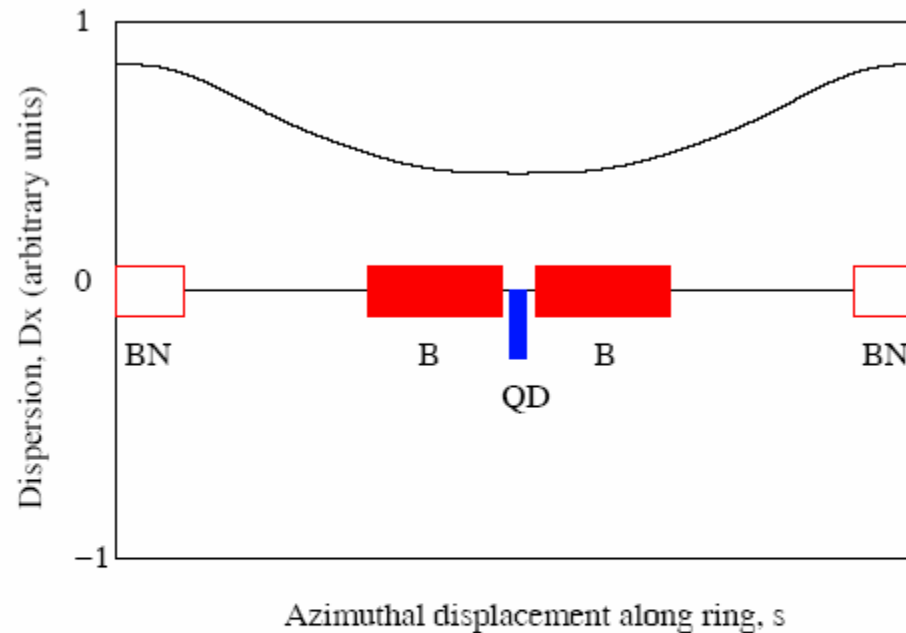


Figure 2: Negative-bend low-momentum-compact lattice. B, BN, and QD denote dipole, negative-bend dipole, and defocusing quadrupole magnets, respectively. The horizontal phase advance across the module is usually below 127° .

Multi-shell crystal in imaginary γ_T lattice

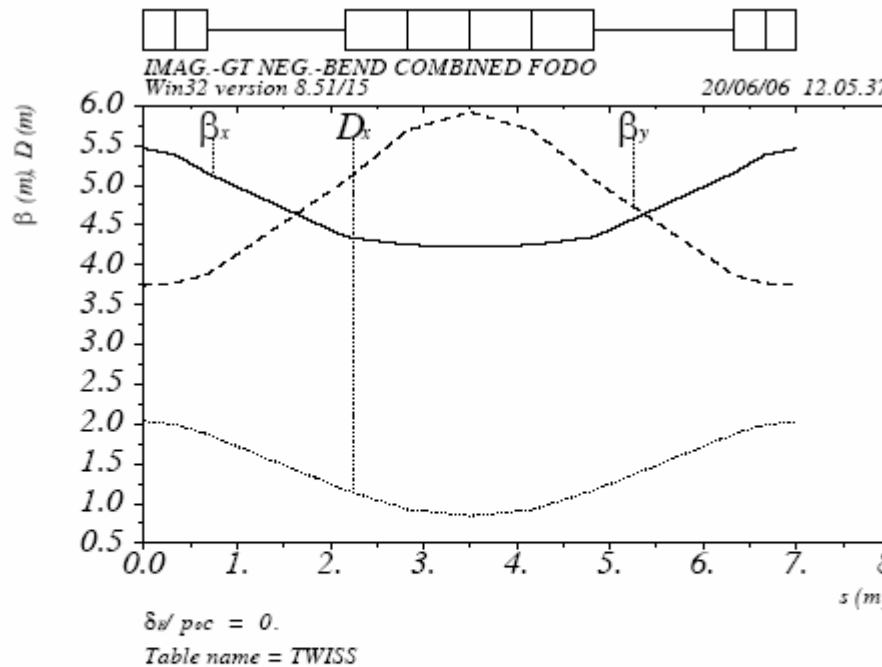


Figure 3: Imaginary- γ_T negative-bend lattice with 87° horizontal phase advance. The middle (positive) bend is of combined-function (dipole and defocusing quadrupole).

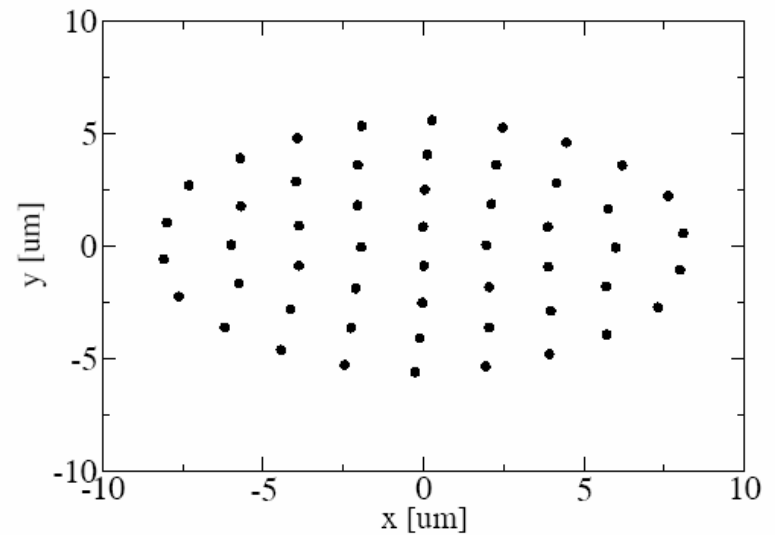


Figure 4: A multi-shell crystalline beam formed with the lattice in Fig. 3 with $\gamma = 1.45$ and density $2.1 \times 10^7/\text{m}$.

Tools for theoretical studies

- Smooth approximation, linearized Coulomb force around equilibrium positions, linearized phonon-spectrum analysis
 - Applicable for 3D crystals
 - Need MD assistance to attain the equilibrium position
 - Maximum solvable system: less than 100 particles per MD cell
 - Analytical formulae for 1D crystal
 - Does not apply on high/imaginary transition lattices
- Phonon spectrum analysis for actual lattices (new progress!)
 - Valid also for high/imaginary transition lattices
 - Solvable only for 1D crystals
- Computer simulation the molecular dynamics method
 - Ewald summation, image charge, simulation of cooling forces ...

Phonon spectrum analysis

- A collection of particles all vibrating around their equilibrium position in the beam rest frame

$$x_\ell = X_\ell + \delta x_\ell, \quad \delta x_\ell = \tilde{x}_\ell \exp[i(\omega t - kZ_\ell)],$$

$$y_\ell = Y_\ell + \delta y_\ell, \quad \delta y_\ell = \tilde{y}_\ell \exp[i(\omega t - kZ_\ell)],$$

$$z_\ell = Z_\ell + \delta z_\ell, \quad \delta z_\ell = \tilde{z}_\ell \exp[i(\omega t - kZ_\ell)].$$
- 6N x 6N matrix for a collection of N particles (linearized force)
- Formalism for 3D crystal under the smooth approximation

$$\begin{aligned} \omega^2 \tilde{x}_\ell &= -i\gamma\omega\tilde{z}_\ell + (\nu_x^2 - \gamma^2)\tilde{x}_\ell + \sum_{n=-\infty}^{\infty} \sum_{m=1}^N \left\{ \left[\frac{1}{R_{\ell mn}^3} - \frac{3(X_\ell - X_m)^2}{R_{\ell mn}^5} \right] [e^{ik(Z_\ell - Z_m - nL)} \tilde{x}_m - \tilde{x}_\ell] \right. \\ &\quad \left. - \frac{3(X_\ell - X_m)(Y_\ell - Y_m)}{R_{\ell mn}^5} [e^{ik(Z_\ell - Z_m - nL)} \tilde{y}_m - \tilde{y}_\ell] - \frac{3(X_\ell - X_m)(Z_\ell - Z_m - nL)}{R_{\ell mn}^5} [e^{ik(Z_\ell - Z_m - nL)} \tilde{z}_m - \tilde{z}_\ell] \right\}, \\ \omega^2 \tilde{y}_\ell &= \nu_y^2 \tilde{y}_\ell + \sum_{n=-\infty}^{\infty} \sum_{m=1}^N \left\{ -\frac{3(X_\ell - X_m)(Y_\ell - Y_m)}{R_{\ell mn}^5} [e^{ik(Z_\ell - Z_m - nL)} \tilde{x}_m - \tilde{x}_\ell] \right. \\ &\quad \left. + \left[\frac{1}{R_{\ell mn}^3} - \frac{3(Y_\ell - Y_m)^2}{R_{\ell mn}^5} \right] [e^{ik(Z_\ell - Z_m - nL)} \tilde{y}_m - \tilde{y}_\ell] - \frac{3(Y_\ell - Y_m)(Z_\ell - Z_m - nL)}{R_{\ell mn}^5} [e^{ik(Z_\ell - Z_m - nL)} \tilde{z}_m - \tilde{z}_\ell] \right\}, \\ \omega^2 \tilde{z}_\ell &= i\gamma\omega\tilde{x}_\ell + \sum_{n=-\infty}^{\infty} \sum_{m=1}^N \left\{ -\frac{3(X_\ell - X_m)(Z_\ell - Z_m - nL)}{R_{\ell mn}^5} [e^{ik(Z_\ell - Z_m - nL)} \tilde{x}_m - \tilde{x}_\ell] - \frac{3(Y_\ell - Y_m)(Z_\ell - Z_m - nL)}{R_{\ell mn}^5} \right. \\ &\quad \left. \times [e^{ik(Z_\ell - Z_m - nL)} \tilde{y}_m - \tilde{y}_\ell] + \left[\frac{1}{R_{\ell mn}^3} - \frac{3(Z_\ell - Z_m - nL)^2}{R_{\ell mn}^5} \right] [e^{ik(Z_\ell - Z_m - nL)} \tilde{z}_m - \tilde{z}_\ell] \right\}, \end{aligned}$$

Analytical results for 1D crystal

$$\omega_1^2 = \frac{1}{2} \left\{ \nu_x^2 + \Omega^2 + \sqrt{(\nu_x^2 + \Omega^2)^2 - 8\Omega^2(\nu_x^2 - \gamma^2 - \Omega^2)} \right\},$$

$$\omega_2^2 = \nu_y^2 - \Omega^2,$$

$$\omega_3^2 = \frac{1}{2} \left\{ \nu_x^2 + \Omega^2 - \sqrt{(\nu_x^2 + \Omega^2)^2 - 8\Omega^2(\nu_x^2 - \gamma^2 - \Omega^2)} \right\},$$

$$\Omega^2 = 2 \sum_{n=1}^{\infty} \frac{1 - \cos(kn/\Lambda)}{(n/\Lambda)^3} \geq 0$$

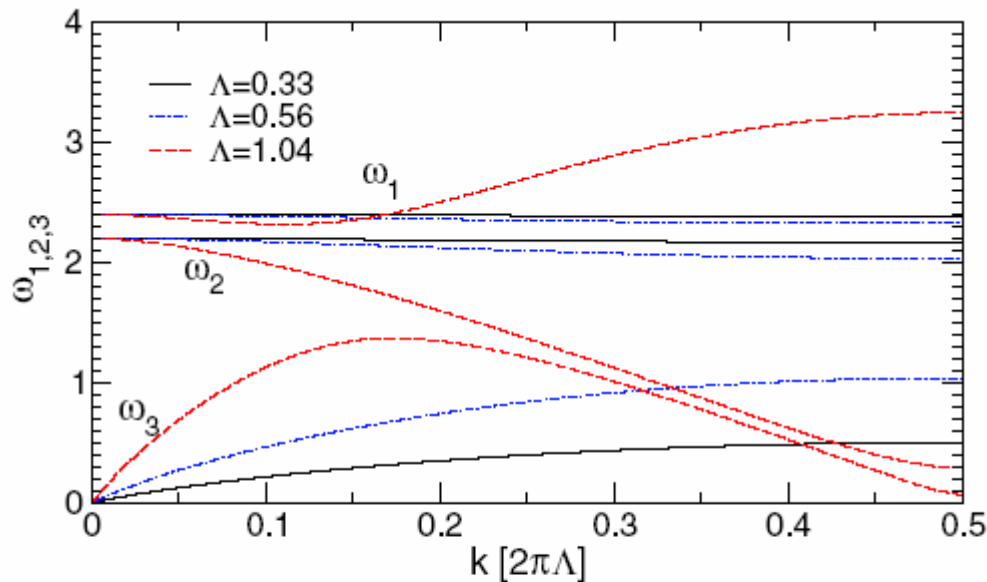


FIG. 1. (Color) Dispersion function evaluated under the smooth approximation of three 1D crystalline beams with $\Lambda = 0.33$, 0.56 , and 1.04 . The horizontal and vertical tunes are $\nu_x = 2.4$ and $\nu_y = 2.2$, respectively, and $\gamma = 1.000016$.

Spectrum under smooth-approximation

- Highest phonon frequency in a crystal $\omega_{\max} \leq \sqrt{\nu_x^2 + \nu_y^2}$.
- High lattice periodicity is preferred $N_{\text{sp}} > 2\sqrt{\nu_x^2 + \nu_y^2}$.
- Low-density crystals can occasionally be formed even when above condition is violated (gaps in the phonon frequency)

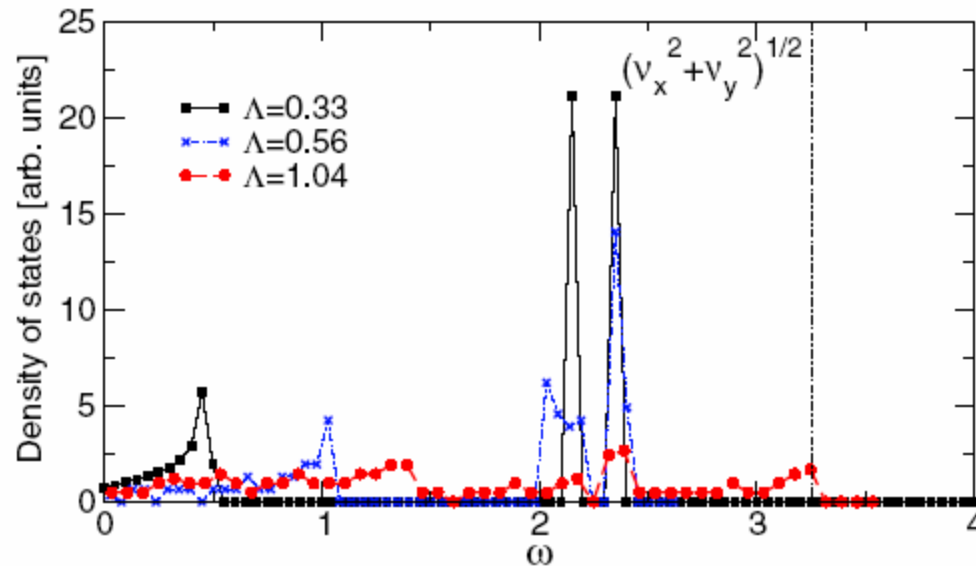


FIG. 2. (Color) Density of states corresponding to Fig. 1 evaluated under the smooth approximation at three beam densities with $\Lambda = 0.33, 0.56, \text{ and } 1.04$.

Phonon theory with actual machine lattice

- Section-wise analysis with phonon approach based on linearized Coulomb force
- One-turn matrix constructed from each section
- Eigenvalue analysis for motion stability of a 1D crystal

$$M = \prod_{i=1}^{N_{lat}} M_i \quad M_y = \prod_{i=1}^{N_{lat}} M_{y,i} \quad M_{xz} = \prod_{i=1}^{N_{lat}} M_{xz,i}$$

$$M_{y,i} = \begin{bmatrix} \cos \omega_{2i} t_i & \frac{\sin \omega_{2i} t_i}{\omega_{2i}} \\ -\omega_{2i} \sin \omega_{2i} t_i & \cos \omega_{2i} t_i \end{bmatrix} \quad M_{xz,i} = \bar{M}_{xz,i} \bar{M}_{xz,i}^{-1}(0)$$

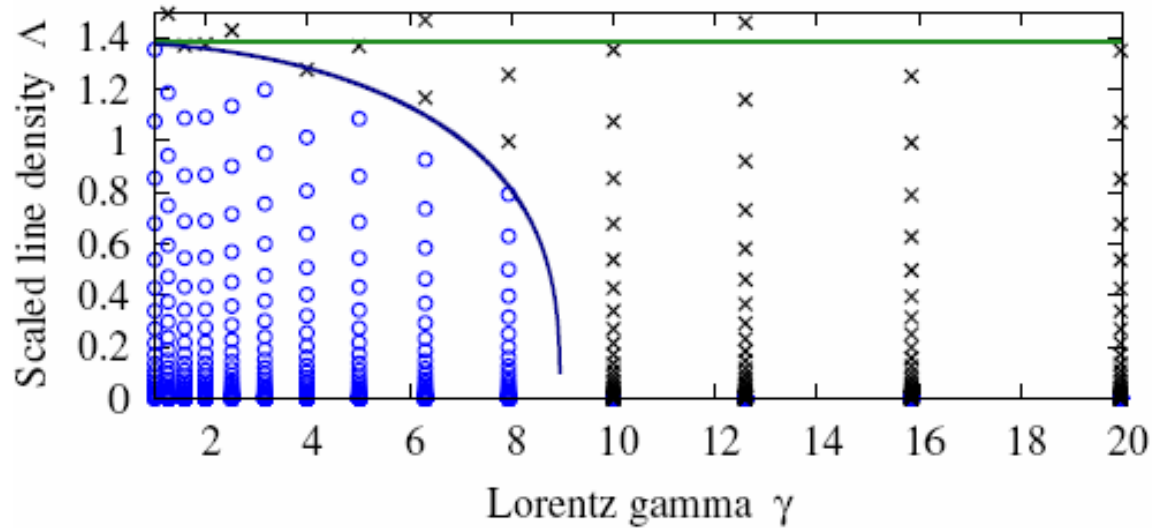
$$\bar{M}_{xz,i} = \begin{bmatrix} e^{i\omega_{1i} t_i} & e^{-i\omega_{1i} t_i} & e^{i\omega_{3i} t_i} & e^{-i\omega_{3i} t_i} \\ i\omega_{1i} t_i e^{i\omega_{1i} t_i} & -i\omega_{1i} t_i e^{-i\omega_{1i} t_i} & i\omega_{3i} t_i e^{i\omega_{3i} t_i} & -i\omega_{3i} t_i e^{-i\omega_{3i} t_i} \\ c_{31} e^{i\omega_{1i} t_i} & -c_{31} e^{-i\omega_{1i} t_i} & c_{33} e^{i\omega_{3i} t_i} & -c_{33} e^{-i\omega_{3i} t_i} \\ c_{41} e^{i\omega_{1i} t_i} & c_{41} e^{-i\omega_{1i} t_i} & c_{43} e^{i\omega_{3i} t_i} & c_{43} e^{-i\omega_{3i} t_i} \end{bmatrix} \quad \bar{M}_{xz,i} = \begin{bmatrix} 1 & 1 & 1 & 1 \\ i\omega_{1i} t_i & -i\omega_{1i} t_i & i\omega_{3i} t_i & -i\omega_{3i} t_i \\ c_{31} & -c_{31} & c_{33} & -c_{33} \\ c_{41} & c_{41} & c_{43} & c_{43} \end{bmatrix}$$

$$c_{31} = \frac{i\omega_{1i} \gamma}{\omega_{1i}^2 - 2\Omega^2} \quad c_{33} = \frac{i\omega_{3i} \gamma}{\omega_{3i}^2 - 2\Omega^2} \quad c_{41} = \frac{-2\Omega^2 \gamma}{\omega_{1i}^2 - 2\Omega^2} \quad c_{43} = \frac{-2\Omega^2 \gamma}{\omega_{3i}^2 - 2\Omega^2}$$

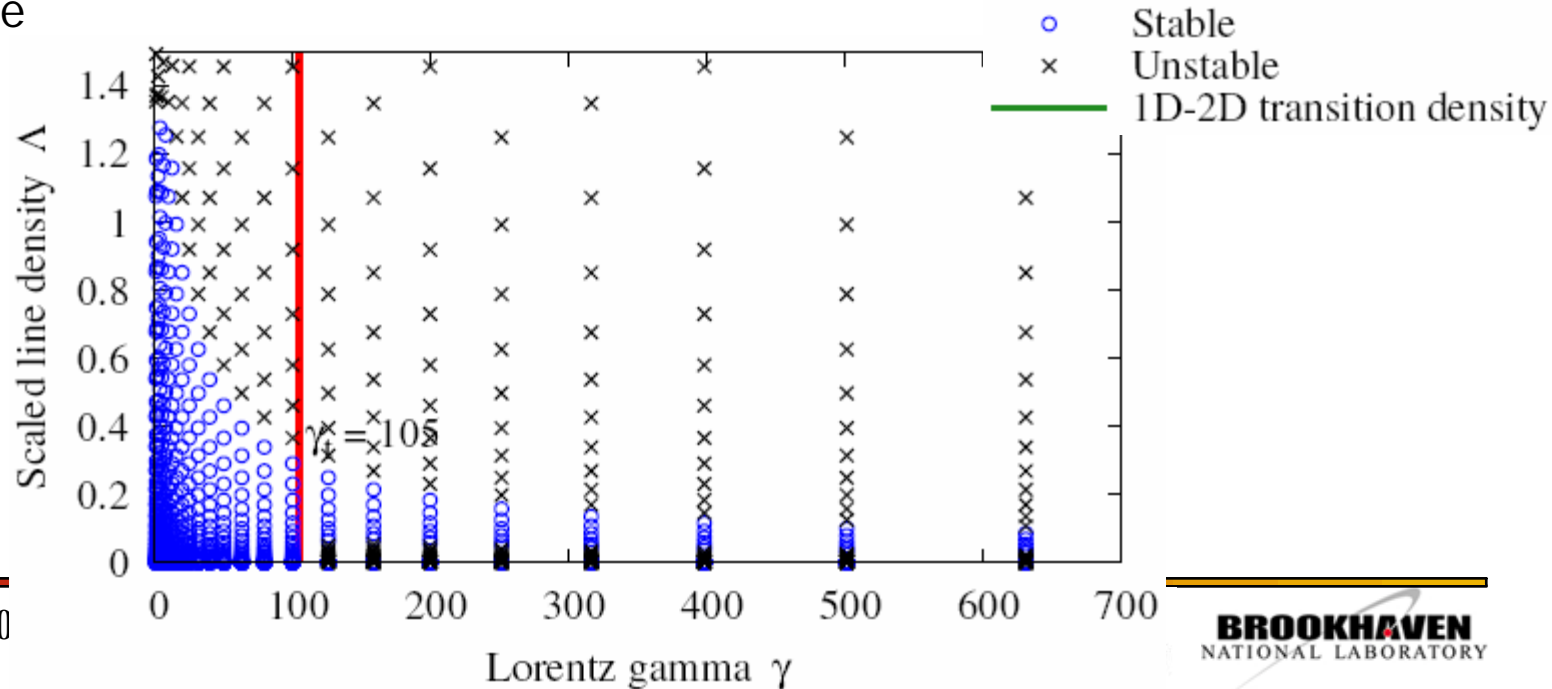
$$\omega_{1i}^2 = \frac{1}{2} \left\{ \nu_{xi}^2 + \Omega^2 + \sqrt{(\nu_{xi}^2 + \Omega^2)^2 - 8\Omega^2 (\nu_{xi}^2 - \gamma^2 - \Omega^2)} \right\}, \quad \omega_{2i}^2 = \nu_{yi}^2 - \Omega^2, \quad \omega_{3i}^2 = \frac{1}{2} \left\{ \nu_{xi}^2 + \Omega^2 - \sqrt{(\nu_{xi}^2 + \Omega^2)^2 - 8\Omega^2 (\nu_{xi}^2 - \gamma^2 - \Omega^2)} \right\}, \quad \Omega^2 = 2 \sum_{n=1}^{\infty} \frac{1 - \cos(kn/\Lambda)}{(n/\Lambda)^3} \geq 0$$

Stability from general-lattice phonon approach

Smooth approximation



General-lattice approach



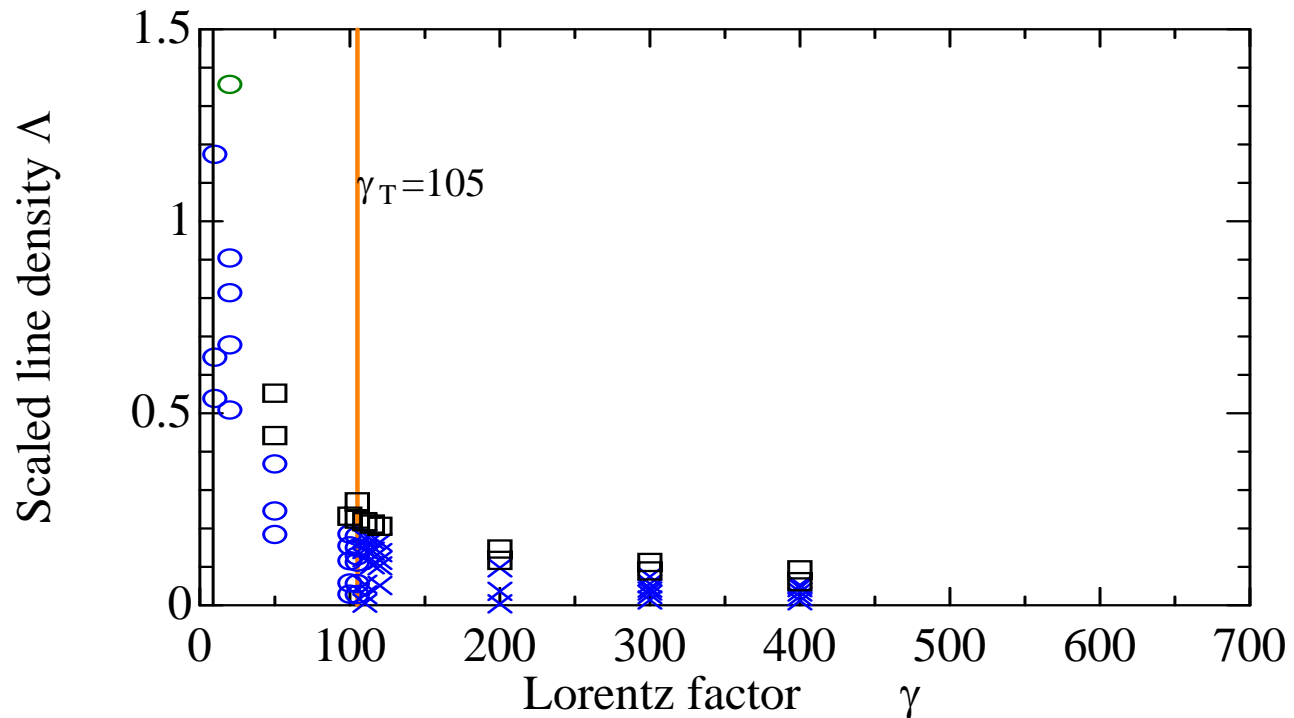
September 11, 20

Indications from the phonon analysis

- When beam energy is below or around tune, $\gamma < v_x, v_y$, multi-shell crystals can be formed
- As energy increases, formation of higher-density (multi-shell) crystals becomes increasingly difficult
- 1D crystals can be formed for $\gamma \gg v_x, v_y$

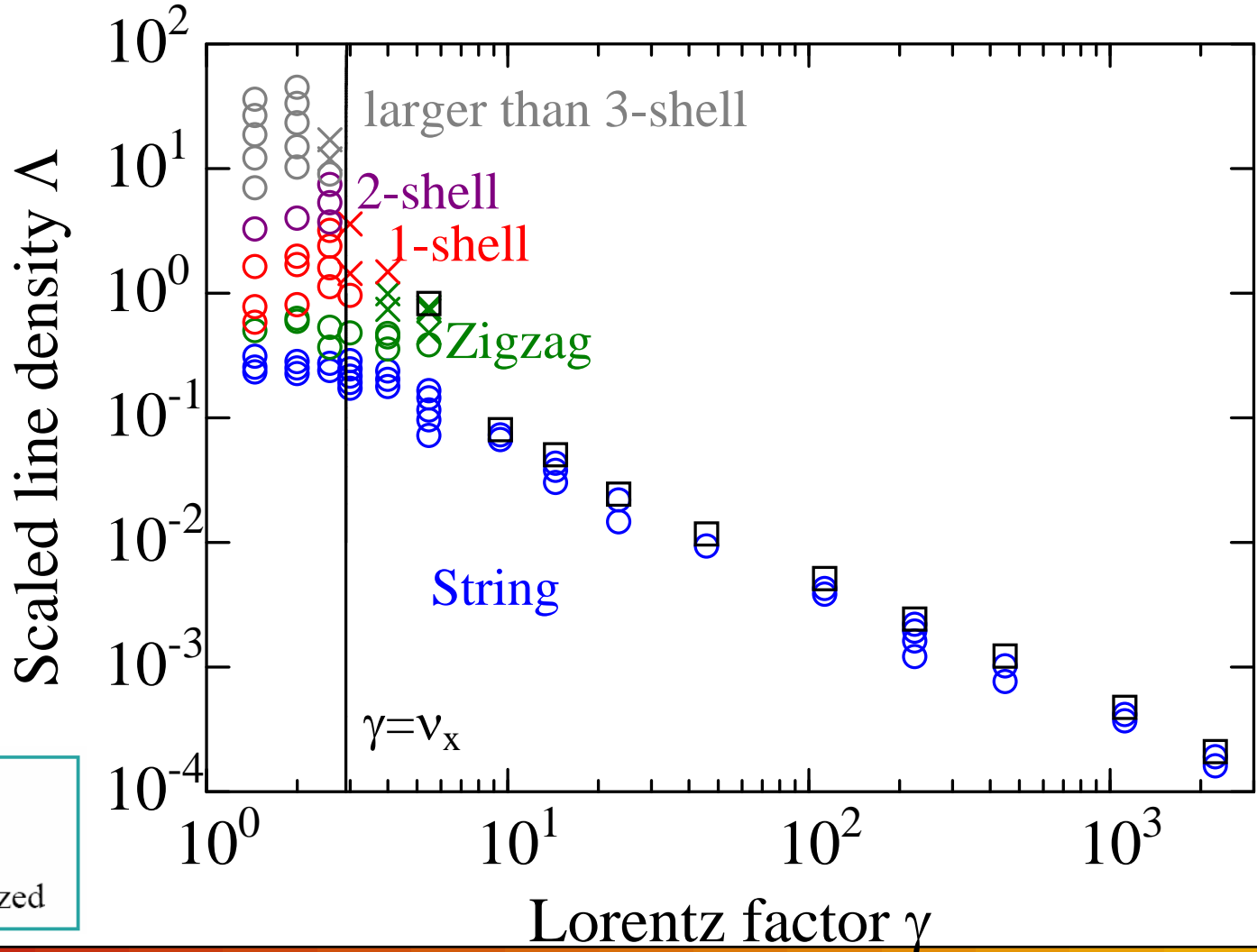
MD study of high energy crystals

- For beam energy (γ) below γ_T , agreement with phonon theory is good
- Beyond γ_T , there is no agreement – no crystals are formed above transition



1D crystal at very high energy

- Imaginary transition energy lattice

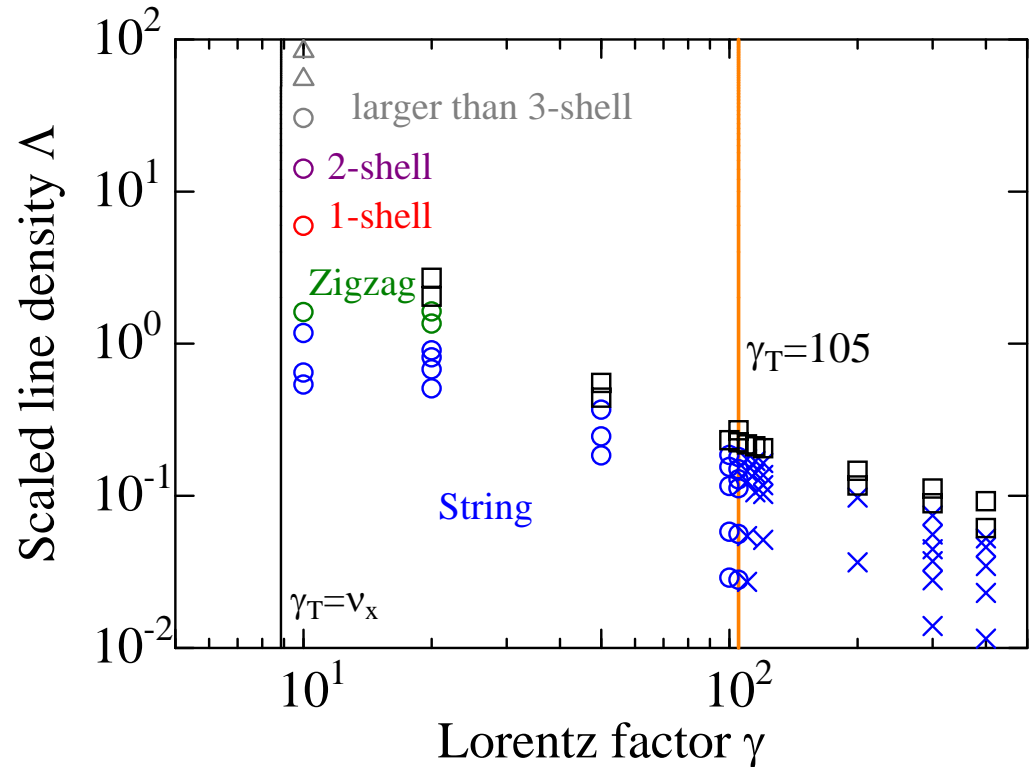
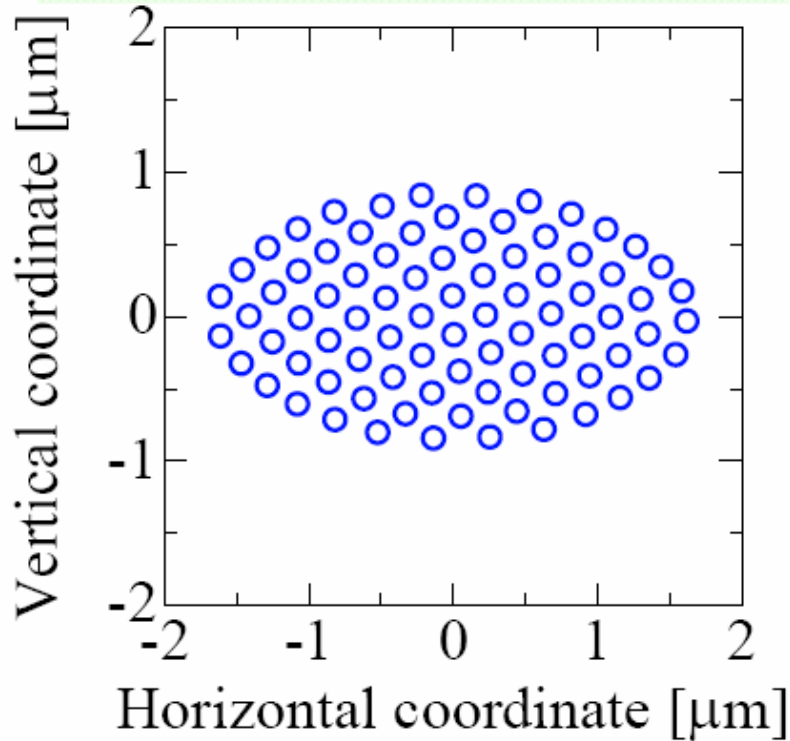


Multi-shell at energies (γ) near tune ν_x

- High transition energy ($\gamma_T=105$, $\nu_x, \nu_y \sim 8.5$) lattice

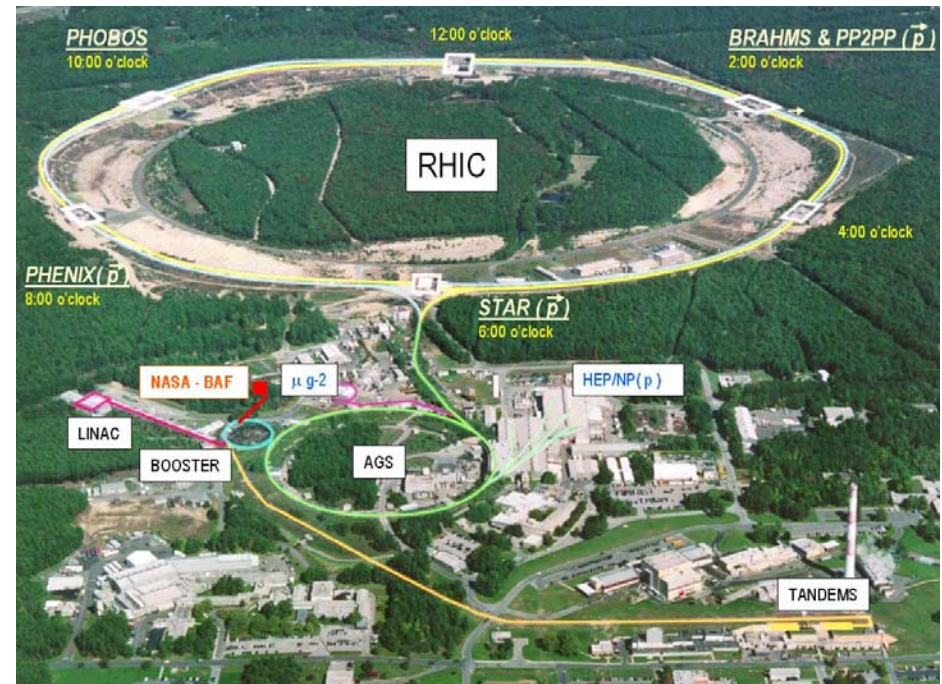
$$\gamma = 10$$

$$N=3.11 \times 10^8 [\text{m}^{-1}]$$



Example 1: Rare ion collider - ordered ions in RHIC-like machine

- Rare ion beams at energy of $\gamma=20$ stored in two rings
- 360 “bunches”, each containing a string of 1 m with 4×10^6 ions
 - Trans. rms amp. at IR $\sim 10^{-6}$ m
 - Mom. spread $\Delta p/p \sim 6 \times 10^{-6}$
- Strong restoring force to resist beam-beam force
 - Incoherent space charge tune shift ~ -1.9
 - Beam-beam parameter ~ 0.38
- Luminosity $3.6 \times 10^{27} \text{ cm}^{-2}\text{s}^{-1}$
(Numerical example: Au on Au)



- Ultra-fast on low intensity ion beam
 - High energy electron cooling
 - Optical stochastic cooling (Tera-Hz)
 - ?

Example 2: Electron-ion collider with an ordered ion beam (Katayama, Moehl on Muses-IR, 2002)

- Rare ion beams (example: Pb) at 180 MeV/u stored in a ring of 180 m circumference
- IR length of 1 m, ion density 1.7×10^4 /m (total 3×10^6)
 - Trans. rms amp. at IR $\sim 6 \times 10^{-6}$ m
 - Mom. spread $\Delta p/p \sim 1.3 \times 10^{-6}$
- Beam-beam force from the electron beam
 - Incoherent ion space charge tune shift ~ -0.25
 - Beam-beam parameter ~ 1
- Colliding electron beam of similar transverse size at IR
- Electron cooling on the ion beam to reach ordering
- Luminosity $1.4 \times 10^{27} \text{ cm}^{-2}\text{s}^{-1}$

Summary and discussions

- Phonon spectrum analysis provides a powerful tool in understanding crystal stability; it complements the molecular dynamics simulations – more to be understood
- Multi-shell crystals can be formed at energies (γ) up to the machine tune (v_x); 1D crystals can be formed to much higher energies using high or imaginary transition-energy lattices
- Multi-shell crystals fail to form at high energies when ($\gamma \gg v_x$), possibly due to sensitivity of the effective transition energy γ_T to the transverse forces between particles
- With suitable cooling, a rare-ion collider may be realized extending to high beam energies
- Demo experiment: Use storage rings with crystal-friendly lattices (like S-LSR) to form ordered beams, and demonstrate colliding crystals passing the ordered beam through crystals formed in a trap

- Our BIGGEST Motivation Is Just To Have Fun -- Okamoto

Yes, we are having fun!

REFERENCES

- [1] J. Wei, A.M. Sessler, EPAC 1998, Stockholm (1998) 862
- [2] J. Wei, X-P. Li, A. M. Sessler, Phys. Rev. Lett., **73**, (1994) 3089
- [3] J. Wei, H. Okamoto, and A.M. Sessler, Phys. Rev. Lett., **80**, (1998) 2606
- [4] J. Wei, X.-P. Li, A.M. Sessler, Proc. 6th Adv. Accel. Conf. (1994) 224
- [5] X.-P. Li, H. Enokizono, H. Okamoto, Y. Yuri, A.M. Sessler, J. Wei, Phys. Rev. ST-AB, **9** (2006) 034201
- [6] K. Okabe, H. Okamoto, Jpn. J. Appl. Phys. **42** (2003) 4584
- [7] I. Hofmann, L. Laslett, L. Smith, I. Haber, Part. Accel. **13** (1983) 145
- [8] R.C. Gupta, J.I. Botman, M.K. Craddock, IEEE Trans. Nucl. Sci. **NS-32** (1985) 2308
- [9] D. Trbojevic, D. Finley, R. Gerig, S. Holmes, EPAC90 (1990) 1536
- [10] V.V. Vladimirski, E.K. Tarasov, Theoretical problems of the ring accelerators, USSR Academy of Science (1955)
- [11] C. Johnstone, E. Keil, A.M. Sessler, and D. Trbojevic, private communications
- [12] H. Okamoto, J. Wei, Phys. Rev. E, **58** (1998) 3817
- [13] J. Wei, H. Okamoto, S. Ochi, Y. Yuri, A.M. Sessler, EPAC (2006) 2841
- [14] I. Meshkov, A. Sidorin, A. Smirnov, E. Syresin and T. Katayama, Inst. of Phys.& Chem. Res. (RIKEN) Report:RIKEN-AF-AC-34 (2002)
- [15] T. Katayama, D. Moehl, RIKEN report (2002)

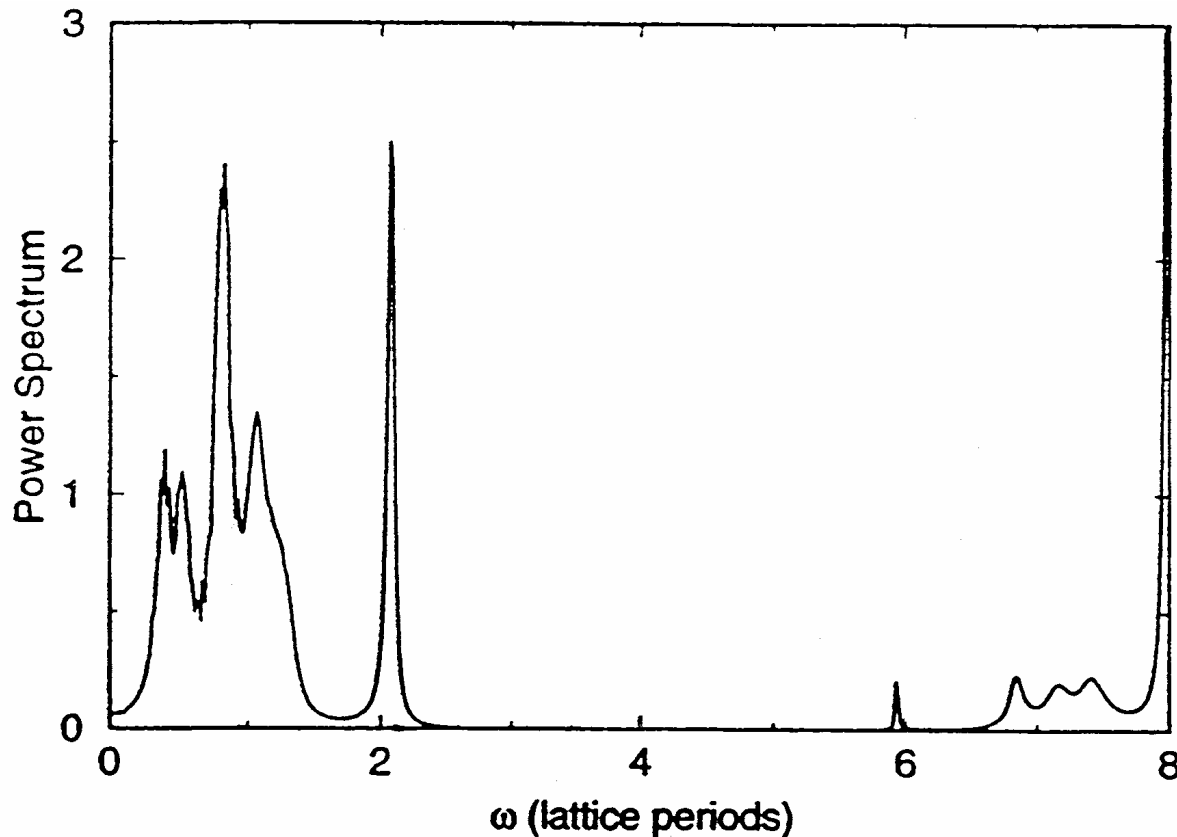
Molecular dynamics methods

- MD cells with longitudinal periodic condition
- Long-range coulomb force -- Ewald-type summation to enhance computational efficiency, considering beam image charge

$$\phi(x_i, x_j) = \frac{1}{r_{ij}} + \frac{4}{L} \int_0^{\infty} \frac{\cosh(2z_{ij}k/L) J_0(2\rho_{ij}k/L) - 1}{\exp(2k) - 1} dk + \frac{2}{L} [\log(\pi b/L) + C]$$

- Integrate EOM with 4th order Runge-Kutta algorithm, potential by 15th order Gauss-Laguerre (later improved to be symplectic)
- Start with a random distribution, and simulate actual cooling process and heating process (or perform artificial ``periodic cooling'' by imposing periodic condition & drift correction for the ground state)

Phonon spectrum of a super-cold beam



- Ring lattice periodicity: 8
- Horizontal tune 2.07; vertical tune 1.38
- Energy $\gamma = 1.1$
- Max. phonon frequency: 3
- Max. allowed tune < 2.83 ;
- Needed for cooling < 2

•X.-P. Li, H. Enokizono, H. Okamoto, Y. Yuri, A.M. Sessler, and J. Wei, "Phonon spectrum and maintenance condition of crystalline beams", Phys. Rev. ST-Accel. Beams, Vol. 9, 034201 (2006).

Closed orbit + phonon modes

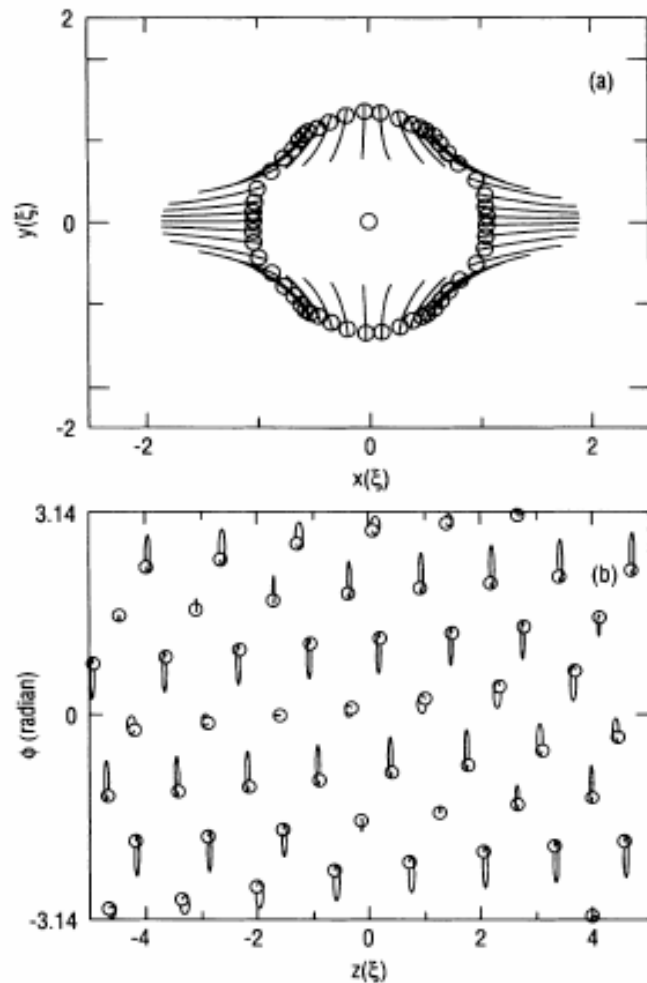


FIG. 1. A 3D structure with particle positions projected (a) into the x - y plane and (b) into the ϕ - z plane, where ϕ is the polar angle. The lattice is a FODO lattice with constant bending with $\nu_x = 2.7$ and $\nu_y = 2.3$, and the particle energy is $\gamma = 1.4$. The total number of particles is 60, and the MD period length is 10ξ . The particles move periodically in time, with the solid lines showing their trajectories and the circles indicating their position at the start and end of the each lattice period.

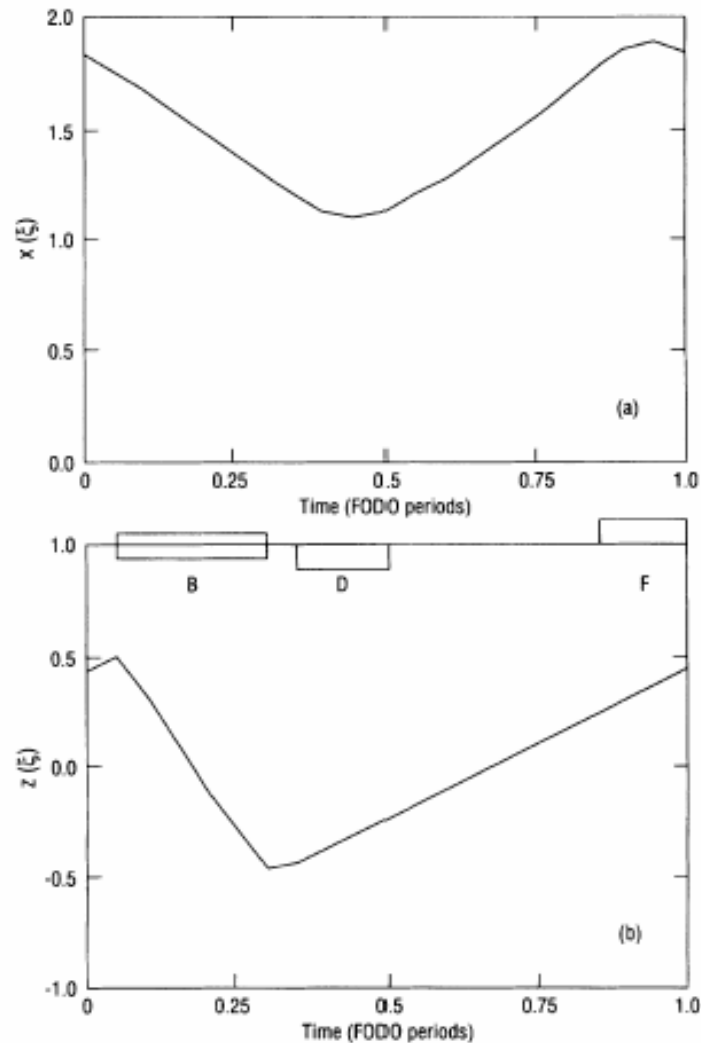
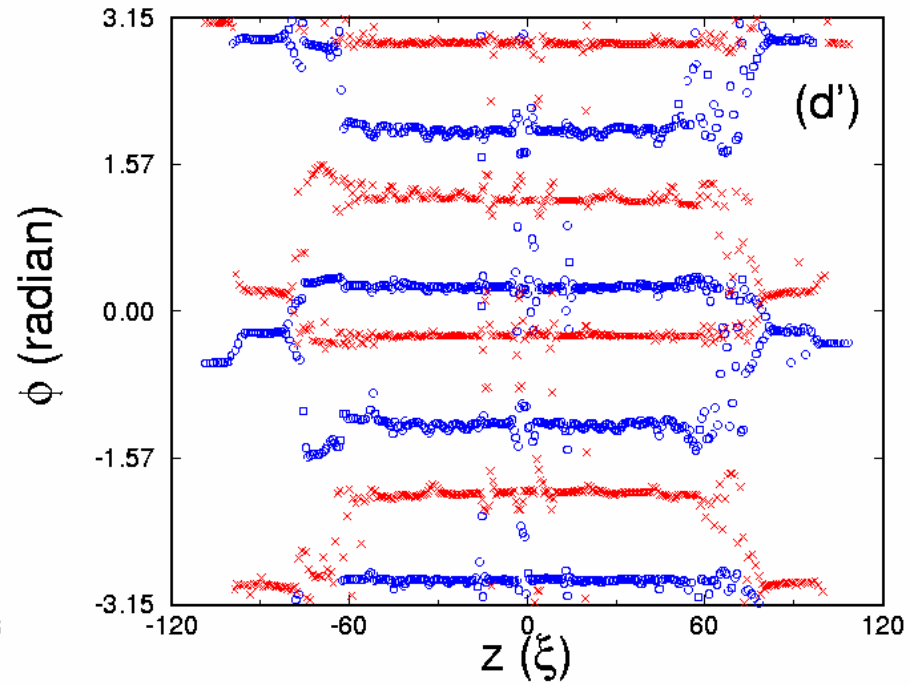
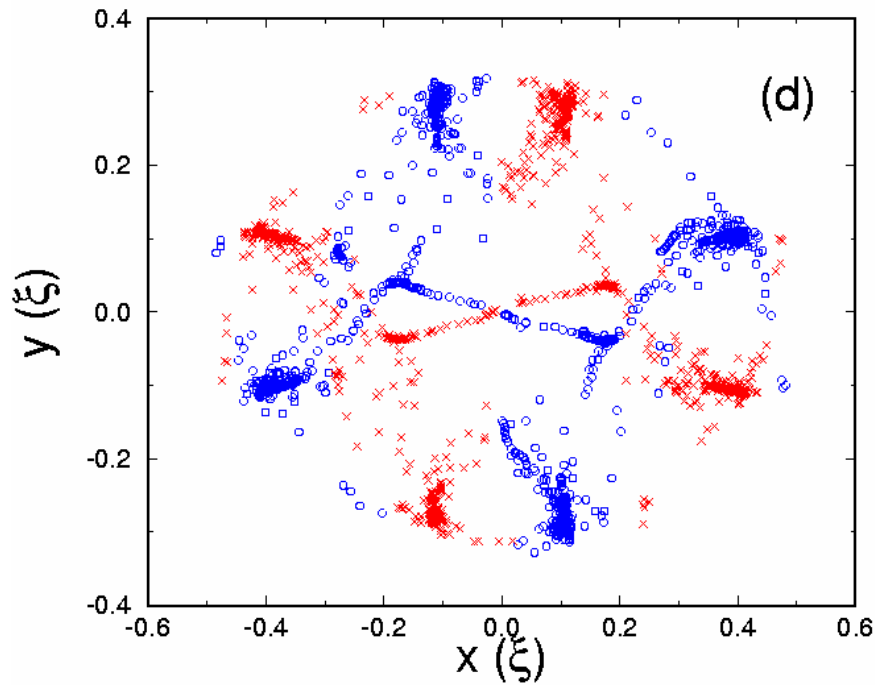


FIG. 2. The effect of shear. In this study $N = 40$, $L = 40\xi$. The cell of one of the particles with largest horizontal displacement (and no vertical displacement) is shown. Motion occurs both (a) in the x direction (breathing) and (b) in the z direction (shear). Lattice components in one of the 10 periods are displayed on the figure: B is a bend section; F is a focusing section; and D is a deforming section.

Colliding crystals -- miss out



- beam-beam tune shift ~ -2.7